

Communication: Vacuum ultraviolet laser photodissociation studies of small molecules by the vacuum ultraviolet laser photoionization time-sliced velocity-mapped ion imaging method

Yang Pan,^{1,2} Hong Gao,¹ Lei Yang,¹ Jingang Zhou,¹ C. Y. Ng,¹ and William M. Jackson^{1,a)}

¹Department of Chemistry, University of California, Davis, Davis, California 95616, USA

²National Synchrotron Radiation Laboratory, University of Science and Technology of China, Hefei, Anhui 230029, People's Republic of China

(Received 8 June 2011; accepted 2 August 2011; published online 15 August 2011)

We demonstrate that the vacuum ultraviolet (VUV) photodissociation dynamics of N₂ and CO₂ can be studied using VUV photoionization with time-sliced velocity-mapped ion imaging (VUV-PI-VMPI) detection. The VUV laser light is produced by resonant sum frequency mixing in Kr. N₂ is used to show that when the photon energy of the VUV laser is above the ionization energy of an allowed transition of one of the product atoms it can be detected and characterized as the wavelength is varied. In this case a β parameter = 0.57 for the N(²D°) was measured after exciting N₂(o¹Π_u, v' = 2, J' = 2) \leftarrow N₂(X¹Σ_g⁺, v'' = 0, J'' = 1). Studies with CO₂ show that when there is no allowed transition, an autoionization resonance can be used for the detection of a product atom. In this case it is shown for the first time that the O(¹D) atom is produced with CO(¹Σ⁺) at 92.21 nm. These results indicate that the VUV laser photodissociation combined with the VUV-PI-VMPI detection is a viable method for studying the one-photon photodissociation from the ground state of simple molecules in the extreme ultraviolet and VUV spectral regions. © 2011 American Institute of Physics. [doi:10.1063/1.3626867]

I. INTRODUCTION

The ion-imaging technique is one of the most important advances in the study of state-selected photodissociation. It was first introduced in 1987 by Chandler and Houston, and then modified as ion velocity imaging in 1997 by Eppink and Parker.^{1,2} The power of this method is that the mass, total kinetic energy release (KER), and angular distributions of the scattered fragment can be obtained from a single image and with the slice variation of the method an energy resolution of the order of 2% can be attained.^{3,4} The method also directly determines the 3D distribution so the signal-to-noise ratio is not degraded by inverting the 2D distribution. In addition the products are detected by ionizing them when their densities are highest before they have had a chance to leave the interaction region. The strong fields that are present then collect them with a very high efficiency. Many of the previous studies on photodissociation of simple molecules using velocity ion imaging employed resonant-enhanced multiphoton ionization (REMPI) to detect the fragments.^{3,5,6} This method uses focused lasers in the interaction region often causing difficulties with interpretation because of multiphoton processes. Ionization of fragments can also be realized with a VUV laser produced by tripling the laser in a Xenon or Krypton cell.^{4,7,8} Resonant enhanced sum or difference-frequency is a better way to produce extreme ultraviolet and VUV radiation because the output intensity is one or two orders of magnitude higher than simply tripling in the rare gases.⁹ Rydberg tagging of the product atoms can also be used but the sensitivity

is much less because the atoms are neutral and a much smaller percentage of the solid angle can be measured.

When one laser at ω_1 is tuned to the two-photon resonance of Kr 4s²4p⁵(²P_{3/2}) 5p'[1/2] (J = 0) \leftarrow 4s²4p⁶(¹S₀) at 212.556 nm (47 046.2 cm⁻¹) is mixed with another visible laser (ω_2) it will produce resonant sum (2 ω_1 + ω_2) and difference (2 ω_1 - ω_2) frequencies by four-wave mixing. Varying ω_2 , 600-900 nm, 16 666.7 to 11 111.1 cm⁻¹, results in a tuning range of the energies for the sum and difference generation of 13.0–13.7 and 9.6–10.3 eV, respectively. In photodissociation dynamics studies one uses one laser for dissociation and another for probing the products. With resonant enhanced four-wave mixing it is conceivable that one or both wavelengths could be used for dissociation of the molecule and the other for detecting the atomic fragment. For H, O, and N atoms with their higher ionization energies, the sum frequency laser is ideal for the single-photon ionization of these atoms from their ground or excited states. Coupling this with time-sliced ion velocity imaging technique will provide a new way to study simple diatomic and triatomic molecules made up of first row atoms.

Preliminary studies of the photodissociation dynamics of N₂ and CO₂ were chosen because of their importance to understanding the chemistry of planetary atmospheres, comets, and the interstellar medium, as well as fundamental photochemical processes.¹⁰

II. EXPERIMENTAL METHODS

The time-sliced ion velocity-mapped imaging apparatus has been described previously in detail.⁶ A beam of the

^{a)}Author to whom correspondence should be addressed. Electronic mail: wmjackson@ucdavis.edu.

sample gas was produced by supersonic expansion through an Evan-Lavie, EL-5-2004 pulsed valve with a 0.2 mm nozzle diameter operated at 30 Hz and a stagnation pressure of 30–50 psi. A pulse width of 20 μ s was used in all of the experiments. The collimated molecular beam and the laser beams all cross at 90° in the interaction region 15 cm from the original nozzle. The ions that are produced were accelerated by fields that change from 140 to 225 V/cm in the velocity mapping ion optics into a 74.7 cm long TOF mass analyzer and projected onto a detector consisting of a 75 mm (Burle Industries, Inc. model ADP 3075FM) dual microchannel plate with a P47 phosphor screen. Sliced images are formed with a 40 ns pulse on the first plate of the MCP detector and are recorded by a CCD camera controlled by the DAVIS 7.2, LaVision software. Gating the nascent ion signals with a SRS SR 245 boxcar and tuning the laser frequency generates photofragment spectra.

The two frequencies ω_1 ($\lambda_1 = 212.556$) and ω_2 (visible) are generated by two Lambda Physik, FL3002 dye lasers pumped by the second harmonic of a Spectra Physics, Inc., Quanta-Ray PRO-290 Nd-YAG laser operated at 30 Hz. One dye laser produces 637.668 nm that is doubled with a β -barium borate (BBO) crystal and summed with 637.668 nm in a second BBO crystal to generate the ω_1 . The ω_1 is then separated from the fundamental and second harmonic with a Pellin-Broca prism, and merged with the ω_2 laser before being focused into the T-shape channel of the four-wave mixing chamber. A pulsed General Valve operating at 30 Hz fills this channel with Kr gas. Typical pulse energies for ω_1 and ω_2 lasers are 0.9 and 5.0 mJ, respectively. According to Hilber *et al.*, the conversion efficiency for resonant sum and difference generation is 10^{-5} and 10^{-3} to 10^{-4} , respectively.⁹ Our conversion efficiency should be higher because the non-linear susceptibility of Kr is higher at 212.556 nm than it is at the 216.6 nm that they used.⁹ The intensities of the ω_1 and ω_2 laser beams are much higher than the intensities of the $2\omega_1 + \omega_2$, $2\omega_1 - \omega_2$, and $3\omega_1$ beams, but their frequencies are not in the one-photon absorption region of ground states of N₂, CO₂, O, and N. Knowing the laser frequencies and using the time-sliced ion velocity-mapped imaging method provides ample tools for deciphering the processes occurring in the interaction region.

III. RESULTS AND DISCUSSION

A. Photodissociation of N₂

The spectrum of the N₂ molecule below 100 nm is complex and many different experimental methods have been used to study its photodissociation in this wavelength region.^{11–13} In our energy regime it is generally agreed that photodissociation occurs via predissociation between the singlet and triplet repulsive states. The photodissociation of N₂ is a good target for our apparatus, because the sum frequency from four-wave mixing reaches the lower energy ranges of the states that lie just below 100 nm that have not been directly studied in the past.

Figure 1 shows the photofragment (PHOFEX) spectra of N⁺ obtained when the sum frequency wavelength in the VUV

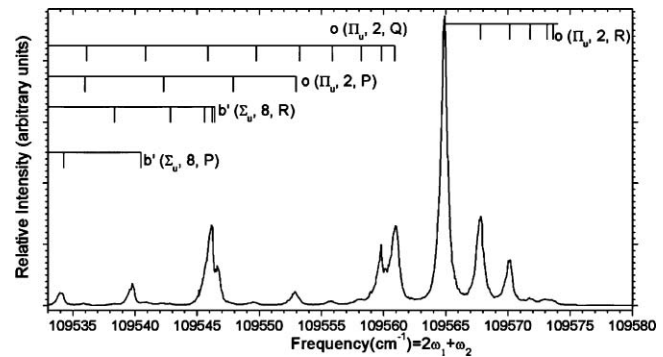


FIG. 1. Photofragment spectrum of N⁺ produced from VUV photoionization of N(2D°) after predissociation of N₂ from 109 530 cm^{−1} to 109 580 cm^{−1}. Pure N₂ was used to produce the supersonic molecular beam. The vertical drop lines identify the J'' levels of the N₂(X¹Σ_g⁺, v'' = 0) state.

is scanned between 109 530 and 109 580 cm^{−1}. This signal can only be observed in the TOF mass spectrum when Kr is present in the T-shaped channel, indicating it comes from the contributions of $2\omega_1 + \omega_2$, $2\omega_1 - \omega_2$, or $3\omega_1$. No significant evidence was found for the occurrence of REMPI process. This spectrum is used to identify the electronic, vibrational, and rotational state of N₂ that is associated with the production of the N⁺ signal. The lines that are observed in the spectrum originate from rotational transitions in the $b'^1\Sigma_u^+ \leftarrow X^1\Sigma_g^+(8,0)$ and $o^1\Pi_u \leftarrow X^1\Sigma_g^+(2,0)$ systems.¹⁴ Figure 2(a) shows the velocity-mapped sliced image of the N₂($o^1\Pi_u$, v' = 2, J' = 2) \leftarrow N₂(X¹Σ_g⁺, v'' = 0, J'' = 1) transition. The total KER spectrum is then obtained from the image, as shown in Fig. 2(b). Only one sharp peak at a kinetic energy of 1.43 eV is present and it is assigned to N(2D°) + N(4S°) products.

A plot of angular distribution of this image fitted with curve corresponding to a $\beta = 0.57$, is shown in Fig. 2(c). The polarizations of the dissociation and ionization lasers all lie parallel to the plane of the detector and along the vertical axis of images in Fig. 2(a). Buijsse and van de Zande have studied the predissociation mechanisms of the $b'^1\Sigma_u^+$ and $e^1\Pi_u$ states of N₂.¹⁵ They photodissociated metastable N₂($a^1\Sigma_g^+$) molecules in a fast beam, and then used a visible laser to excite these molecules to higher vibrational levels of these states. Their results showed a strong dependence of the values of the anisotropy parameter β on the character of transition. Using the theory that they developed we have calculated the expected β value for dissociation through a $^3\Pi_u$ state Hund's

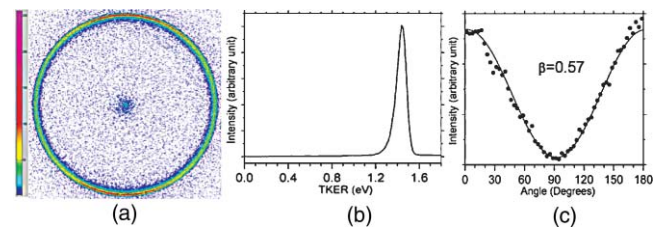


FIG. 2. Sliced raw image, total kinetic energy release spectrum and the angular distribution for predissociation channel N(4S°) + N(2D°) produced after VUV excitation of N₂($o^1\Pi_u$, v' = 2, J' = 2) \leftarrow N₂(X¹Σ_g⁺, v'' = 0, J'' = 1): (a) sliced raw image; (b) total kinetic energy release spectrum; (c) experimental angular distribution (solid dots) and fitted curve (solid line) corresponding to a β of 0.57. A neat supersonic beam of N₂ gas at room temperature is used.

case a coupling gives a value of 0.5. This is in reasonable agreement with the observation. To really test the various theoretical approaches we are currently measuring the variation of β with J as a function of the initial excitation of the ro-vibronic excited state. The N_2 study shows that an unfocused tunable VUV laser can be used to both photodissociate the molecule and detect the metastable product when the photon energy of the VUV laser is above the threshold for ionization of the metastable $N(^2D)$ and $N(^2P)$ product atoms via an allowed transition.

B. Photodissociation of CO_2

The photochemistry of CO_2 in the deep VUV region is important to understanding the atmosphere of Mars.¹⁶ Lawrence has shown that 50% of the quantum yield is $O(^3P) + CO (a^3\pi)$ and other triplet states of CO at ~ 920 nm but no direct determination of the other channels $O(^1D)$ or $O(^1S) + CO (X^1\Sigma)$ have been reported.¹⁷ There is enough energy at the $2\omega_1 + \omega_2$, sum frequency in this region to ionize the $O(^1D)$ and $O(^1S)$ atoms to the $O^+(^4S_{3/2})$ state but it is spin forbidden. A further complication to a study of CO_2 molecules is that it absorbs at both the difference and the sum frequencies of the resonant four wave mixing wavelengths. We estimate that the relative probabilities of dissociation at $(2\omega_1 - \omega_2)$: $(2\omega_1 + \omega_2)$: $3\omega_1$ is 0.02-0.2:1.00:0.04 based upon the product of the absorption coefficients and the laser energies so the sum frequency should dominate the dissociation.

Figure 3(a) shows an image of the $O(^1D)$ atom obtained in the photodissociation of CO_2 at 92.207 nm, which is at the autoionization line of $O(^1D_2) \rightarrow 2s^2 2p^3 (^2D_{3/2}) 3d^1 D_2$. The $P(E_T)$ derived from this slice image is shown in Fig. 3(b). The probe laser had to be scanned over the line when taking the image to take into account the Doppler profile of the line. No signal was observed when the laser was off resonance. The image is characterized by many concentric anisotropic rings, corresponding to the vibrational states of the dissociative CO product that is similar to the results obtained earlier in the photodissociation of CO_2 at 157 nm.^{17,18} The observed total KER extends to 5.5 eV. If photodissociation is occurring at $2\omega_1 - \omega_2$ of $79\,734.2\,cm^{-1}$, the maximum KER should be ~ 2.4 eV for the $O(^1D) + CO(^1\Sigma^+)$ channel but this would imply that dissociation at the higher energies have a lower probability than one expects. To obtain the higher available energies, the resonant sum or tripling frequencies at $108\,451.5$ and $141\,139.3\,cm^{-1}$ must be involved with the maximum KER of 6.1 and 10.2 eV, respectively. The maximum observed KER is 5.5 eV and the expected dissociation probabilities of $(2\omega_1 + \omega_2)$: $3\omega_1$ is 1.00:0.04, it is more likely that the resonant sum frequency is responsible for the observed dissociation.

In summary, we have shown that unfocused VUV laser formed by resonance enhanced four-wave mixing can be used to study photodissociation of small molecules in this region. In the N_2 studies the products are detected because the energy of the VUV laser is above the energy needed for direct ionization of the metastable atoms via an allowed transition. But in the case of CO_2 the product atoms are ionized using an autoionization resonance. The success of the method depends

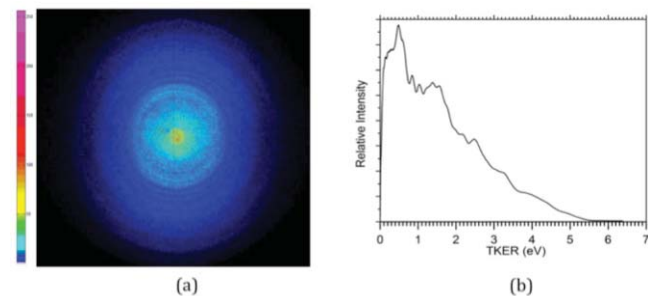


FIG. 3. Photodissociation of CO_2 at $108\,451.5\,cm^{-1}$. Oxygen atoms in the $O(^1D_2)$ state are detected via the autoionization transition $2s^2 2p^3 (^2D_{3/2}) 3d^1 D_2 \leftarrow O(^1D_2)$. (a) The sliced image and (b) the $P(E_T)$ derived from the image. The structure is reproducible but complicated.

on the use of the slice imaging method to provide the sensitivity and selectivity to determine the identity and the angular and velocity distribution of the products.

Future studies are planned that will introduce a second VUV laser that can be used to exploit these observations by being able to independently vary the wavelength of the detection and photolysis lasers. This will allow us to systematically study this very high-energy region where many of the excited states are directly connected to metastable atoms and molecules in the final states.

ACKNOWLEDGMENTS

Y. Pan, H. Gao, Jingang Zhou, and W. M. Jackson acknowledge the support of the Chemistry Division of the National Science Foundation under Grant No. CHE-0957872. H. Gao and C. Y. Ng acknowledge the support of AFOSR under Grant No. FA9550-06-1-0073 and the NASA Planetary Atmospheres Program with Grant No. 07-PATM07-0012. Partial support by the DOE on Contract No. DEFG02-02ER15306 and the NSF Experimental Physical Chemistry Program on Grant No. CHE 0910488 is also acknowledged.

¹X. M. Yang and K. P. Liu, *Modern Trends in Chemical Reaction Dynamics: Experiment and Theory* (World Scientific Publishing Co. Pte. Ltd., Singapore, 2004).

²D. W. Chandler and P. L. Houston, *J. Chem. Phys.* **87**, 1445 (1987); A. Eppink and D. H. Parker, *Rev. Sci. Instrum.* **68**, 3477 (1997).

³D. Townsend, M. P. Miniti, and A. G. Suits, *Rev. Sci. Instrum.* **74**, 2530 (2003).

⁴*Imaging in Chemical Dynamics*, edited by A. G. Suits and R. E. Continetti (American Chemical Society, Washington, DC, 2001), p. 103.

⁵M. L. Lipciuc, A. J. van-den-Brom, L. Dinu, and M. H. M. Janssen, *Rev. Sci. Instrum.* **76**, 123103 (2005).

⁶J. G. Zhou, K. C. Lau, E. Hassanein, H. F. Xu, S. X. Tian, B. Jones, and C. Y. Ng, *J. Chem. Phys.* **124**, 034309 (2006).

⁷W. Ubachs, L. Tashiro, and R. N. Zare, *Chem. Phys.* **130**, 1 (1991).

⁸W. M. Jackson, D. D. Xu, R. J. Price, K. L. McNeely, and I. A. McLaren, *ACS Symp. Ser.* **770**(7), 103 (2000); D. D. Xu, R. J. Price, J. H. Huang, and W. M. Jackson, *Zeits. für Physik. Chemie* **215**, 253 (2001); W. M. Jackson and D. D. Xu, *J. Chem. Phys.* **113**, 3651 (2000).

⁹G. Hilber, A. Lago, and R. Wallenstein, *J. Opt. Soc. Am. B* **4**, 1753 (1987).

¹⁰H. Kato and M. Baba, *Chem. Rev.* **95**, 2311 (1995).

¹¹H. Helm and P. C. Cosby, *J. Chem. Phys.* **90**(8), 4208 (1989); M. O. Vieitez, T. I. Ivanov, W. Ubachs, B. R. Lewis, and C. A. de-Lange, *J. Mol. Liq.* **141**, 110 (2008); S. T. Pratt, P. M. Dehmer, and J. L. Dehmer, *J. Chem. Phys.* **81**, 3444 (1984); S. T. Pratt, E. D. Poliakoff, P. M. Dehmer, and J. L. Dehmer, *ibid.* **78**, 65 (1983).

¹²H. Helm and P. C. Cosby, *J. Chem. Phys.* **90**(8), 4208 (1989); C. W. Walter, P. C. Cosby, and H. Helm, *ibid.* **99**(5), 3553 (1993).

¹³J. P. Sprengers, W. Ubachs, and K. G. H. Baldwin, *J. Chem. Phys.* **122**, 144301 (2005); M. O. Vieitez, T. I. Ivanov, W. Ubachs, B. R. Lewis, and C. A. de-Lange, *J. Mol. Liq.* **141**, 110 (2008).

¹⁴K. Yoshino, Y. Tanaka, P. K. Carroll, and P. Mitchell, *J. Mol. Spectrosc.* **54**, 87 (1975); J. Y. Roncin, J. L. Subtil, and F. Launay, *ibid.* **188**, 128 (1998).

¹⁵B. Buijsse and W. J. van der Zande, *J. Chem. Phys.* **107**(22), 9447 (1997).

¹⁶M. B. McElroy and D. M. Hunten, *J. Geophys. Res.* **75**, 1188 (1970).

¹⁷G. M. Lawrence, *J. Chem. Phys.* **56**, 3435 (1972).

¹⁸Z. C. Chen, F. C. Liu, B. Jiang, X. M. Yang, and D. H. Parker, *J. Phys. Chem. Lett.* **1**, 1861 (2010).